Turbulence modelling for flotation cells based on piezoelectric sensor measurement data

Jun Meng[*1], Weiguo Xie[1], Erico Tabosa[2], Kym Runge[1,2], Dee Bradshaw[1]

1. Julius Kruttschnitt Mineral Research Centre, 40 Isles Road, Indooroopilly, QLD 4068, Australia
2. Metso Process Technology & Innovation, 1 Technology Court, QLD 4069, Australia

Abstract

Turbulence is an important factor that affects flotation performance, which needs to be incorporated into flotation models. However, the measurement of turbulence in industrial flotation cells is difficult because of the highly abrasive and aggressive slurry environment. This has made the development and validation of models incorporating turbulence difficult. The development of a measurement methodology based on the piezoelectric vibration sensor (PVS) has enabled the measurement of kinetic energy fluctuation in flotation cells. In the study presented in this paper, the PVS was first applied to a sugary water-air two phase mixture in a 3 m^3 pilot flotation cell, and then to a Metso 3 m^3 flotation test rig with magnetite/silica slurry and air, to collect turbulence data. An orthogonal experimental design was used for both sets of tests, with different impeller speeds, air flow rates, cell level (aspect ratio) and sugar concentration (viscosity) as input hydrodynamic parameters. From the measurement data collected in the two cells, the volume of the turbulence zone could be modelled; from this, the turbulence distribution in the flotation cells could be predicted. The models were validated by comparing the predicted with the experimental results.

Keywords: turbulence, piezoelectric sensor, modelling, flotation

1. Introduction

Turbulence has long been considered an important factor affecting flotation performance: it impacts on micro-processes such as solid suspension, air dispersion, bubble-particle collision and entrainment (Fallenius,1987; Schubert,1999; Xia, Rinne & Grönstrand,2009; Tabosa, Runge & Holtham,2012). Consequently, the turbulence distribution in flotation cells is of interest to researchers. Tabosa, Runge and Holtham(2014) investigated the distribution of turbulence and its influence on flotation performance in a 3 m^3 flotation cell. They found that the collection zone flotation rate constant can be related to the size of the turbulence zone. By increasing the depth of slurry in a standard Leeds flotation cell, Morris and Matthesius(1988) studied the influence of turbulence level on bubble-particle attachment and beneficiation efficiency in coal flotation over a particle size range from 36 to 600μm. They found that for particle sizes larger than 150μm, bubble-particle attachment was affected by the turbulence level. This was resolved by changing the cell aspect ratio and extending the quiescent zone to allow efficient recovery of particles up to 350 μm in size. Tabosa, Runge and Duffy(2013) studied the coarse particle recovery in a Metso 3 m^3 Reactor Cell System(RCS) flotation cell and concluded that a better coarse particle recovery rate could only be attained by operating the flotation cell to maximise the froth recovery, which meant using a shallow or zero froth depth and minimum turbulence at the pulp froth interface. The turbulence intensity was modified by using different impeller sizes, design, tip speed and cell aspect ratio in their research.

All this previous research indicates that turbulence level and distribution play an important part in flotation performance, and that it would be useful to correlate turbulence related parameters with hydrodynamic parameters. However, the study of turbulence in flotation cells, especially industrial ones, has been difficult because of the highly abrasive and aggressive slurry environment. Although many turbulence measurement techniques exist, such as Constant Temperature Anemometry (CTA) (Sherif,1998), Laser Doppler Anemometry (LDA) (Morud & Hjertager,1996), Particle Image Velocimetry (PIV) (Grant & Smith,1988), Positron Emission Particle Tracking (PEPT) (Ngoepe *et al.*,2013) and the Aeroprobe(Brennan *et al.*,2007), none of these can be used to measure turbulence in industrial flotation cells. Fortunately researchers have made efforts to solve this problem. First developed by Tabosa, Runge and Holtham(2012) and then further investigated by Meng, Xie, *et al.*(2014), the piezoelectric vibration sensor (PVS) has been proven to be a suitable tool for turbulence measurement in flotation cells. The PVS has been tested in a three phase industrial flotation cell and preliminary results have demonstrated that the change in kinetic energy fluctuation can be captured by the sensor (Meng, Tabosa, *et al.*,2014). This has enabled the collection of turbulence datasets which can be used to model turbulence distribution in flotation cells.

Corresponding author: Julius Kruttschnitt Mineral Research Centre, University of Queensland, PhD. Scholar, 40 Isles Road Indooroopilly, QLD 4068, Australia. Phone: +61733655823. Email: j.meng2@uq.edu.au

In the research work described in this paper, the PVS was successively applied in a pilot 3 m³ cell filled with sugary water and air, at the Julius Kruttschnitt Mineral Research Centre (JKMRC) of the University of Queensland; and a Metso 3 m³ RCS flotation test rig filled with slurry and air. The cells were operated at different impeller speeds, air flow rates, cell aspect ratio and fluid viscosity. Turbulence level readings from the PVS measurements were recorded and datasets for calculating turbulence distribution were established. The aim was to identify the impacts of different hydrodynamic parameters on the turbulence distribution. To single out the effect of each hydrodynamic parameter, an orthogonal experimental design was used and the range of achieved impacts on the turbulence parameters was analysed for each hydrodynamic parameter. In previous research, the modelling of turbulence was to provide a calculation basis for Computational Fluid Dynamic (CFD) simulation (Menter,1993; Balaras & Benocci,1994; Lu, Rutland & Smith,2007). In this research, the turbulence distribution model was established from the PVS measurement data with hydrodynamic parameters as input. The results are presented below.

2. Experimental equipment and testing rigs

2.1 JKMRC 3 m³ pilot cell

The JKMRC cell used in the tests was the one used by Sanwani(2006) to measure gas dispersion. It was a 3 m³ rectangular glass cell 163 cm in length and width and 117 cm in height. The height of the stator was 33.3 cm. A schematic drawing of the cell is depicted in Figure 1. The flotation cell was operated with water-air only. Water viscosity was modified by adding sugar at different concentrations.
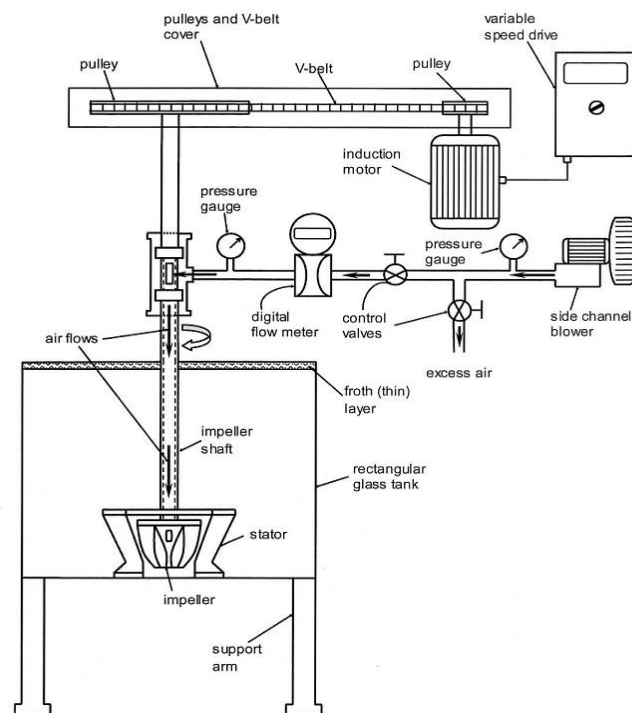

Figure 1. Schematic drawing of the 3 m³ cell (Sanwani,2006)

The impeller was driven by a pulley and V-belt which was connected to a variable speed motor. The impeller speed could be varied from as low as 100 rpm to as high as 300 rpm. The air inlet pipe was connected to an air blower to supply air to the flotation cell. The air flow rate could be read through a digital air flow meter installed onto the air inlet pipe. Two control valves could be used in combination to adjust the inlet air pressure and flow rate. The top and side views of the cell are shown in Figure 2.

<table>
<tr><td>(a). Top view of the cell</td><td>(b). Side view of the cell</td></tr>
</table>

Figure 2. Top and side view of the 3 m^3 cell

2.2 Metso 3 m^3 RCS flotation test rig

The Metso 3 m^3 RCS flotation test rig (Figure 3) contained a cylindrical flotation cell that could be operated in both open circuit and recycle mode (i.e., recycling both concentrate and tail). Herein, however, the cell was operated in batch mode (no feed or discharge flow). The cell was 145 cm in height and 170 cm in diameter. A 52 cm-diameter stator with a height of 30.5 cm was mounted 1 cm above the bottom of the cell. The 33 cm-diameter impeller was driven by a variable speed motor and could be operated at speeds as high as 420 rpm. The air blower was connected to a hose that supplied air to the cell at an adjustable air rate. The flotation cell was operated with a slurry comprised of silica and magnetite (assaying 1.6% magnetite), with a solids concentration of about 20% by weight and particle size P_{80} of 180 µm.
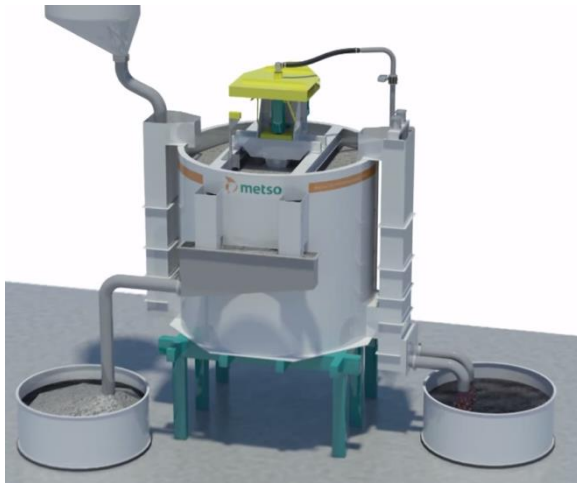
<table>
<tr><td>(a)   Schematic diagram</td><td>(b)   On site side view</td></tr>
</table>

Figure 3 Metso 3 m^3 RCS flotation test rig

2.3 PVS measurement tool

The piezoelectric sensor consisted of a piezoelectric film which was glued to the end of a metal rod, as shown in Figure 4(a). The sensor converted mechanical vibrations to electrical voltage signals. It was connected to a LabJack U3HV data acquisition box (Figure 4(b)) which sampled the electrical signal produced by the piezoelectric film. The sampled data were then transferred to a laptop and processed by LabVIEW software designed to analyse the signal (Figure 4(c)).
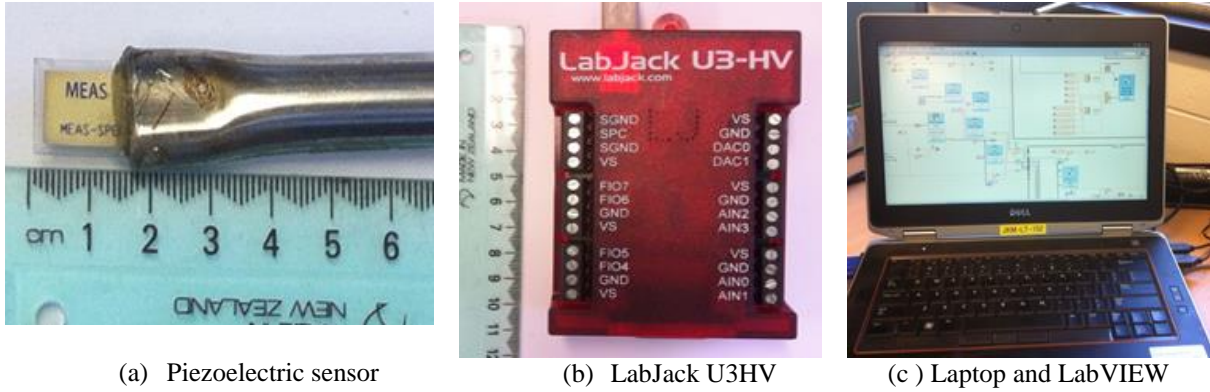
(a) Piezoelectric sensor   (b) LabJack U3HV   (c) Laptop and LabVIEW

Figure 4. PVS measurement components

To use the sensor in both the JKMRC cell and the Metso cell, the rod to which the sensor was glued was housed within a longer metal tube. The tube was fitted to a square metal plate which could be fixed to the upper frame or mesh of the cells by G-clamps, as shown in Figure 5. The measurement position could be adjusted by moving the metal tube up or down and changing the position of the plate.
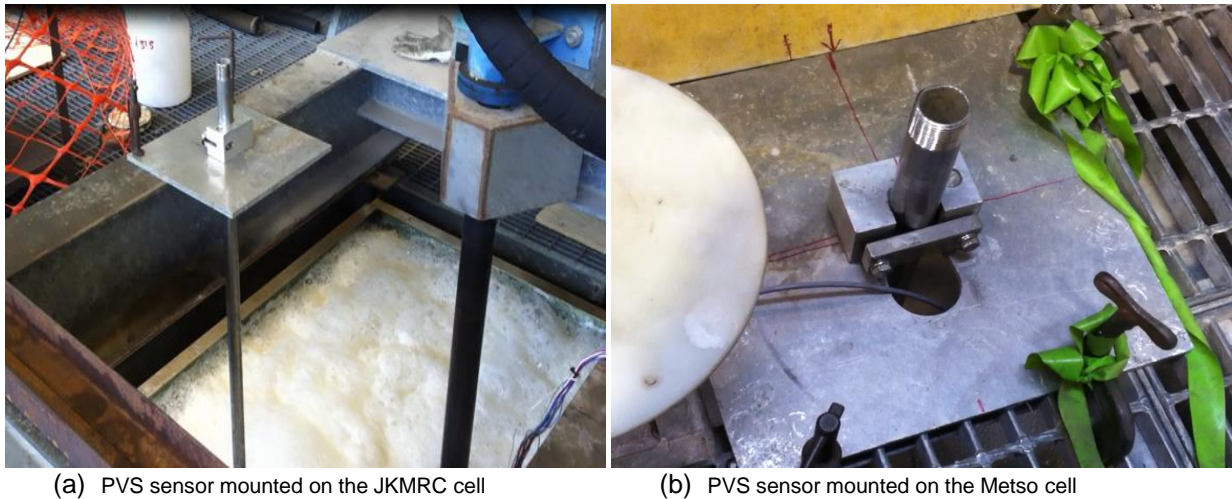

(a) PVS sensor mounted on the JKMRC cell   (b) PVS sensor mounted on the Metso cell

Figure 5. Metal plate and tube to fix the PVS sensor to the cell

3. Experimental design

The aim of the experiments was to develop turbulence distribution models for both of the flotation cells and to quantify the impact of different hydrodynamic parameters on turbulence. To achieve this objective, an orthogonal experimental design (Keppel,1991) was used to calculate the values of the input parameters used for each experiment. The key advantage of orthogonal experimental design is that it allows for the effectiveness of many factors to be tested simultaneously with many fewer tests than all combinations of the factors.

3.1 Experimental design for the JKMRC cell

Four hydrodynamic parameters were selected for the JKMRC cell: the impeller speed, the air flow rate, the cell water level and the sugar concentration. The five factors and four levels L16 orthogonal array table (Keppel,1991) was chosen to design the experiments as it was the closest to the requirement. Four levels were assigned to each parameter. Table 1 shows the values at each level for each parameter and Table 2 the 16 experiments that were orthogonally designed with L16. Table 3 shows the control group of 4 experiments which were used to test the capability of the turbulence distribution model to do predictions.

Table 1. Values of different levels for the parameters

|	Water level (cm)	Sugar concentration (wt%)	Impeller speed (rpm)	Superficial gas velocity J_g (cm/s)
Level 1	70	0	150	0.6
Level 2	85	2	190	0.8
Level 3	100	4	230	1
Level 4	106	6	270	1.2

Table 2. Orthogonally designed experiments from L16

Experiment number	Water level	Sugar concentration level	Impeller speed level	Air flow rate level
1	1	1	1	1
2	2	1	3	4
3	3	1	4	2
4	4	1	2	3
5	1	2	3	3
6	2	2	1	2
7	3	2	2	4
8	4	2	4	1
9	1	3	4	4
10	2	3	2	1
11	3	3	1	3
12	1	4	2	2
13	4	3	3	2
14	2	4	4	3
15	3	4	3	1
16	4	4	1	4

Table 3. Control group experiments

Experiment number	Water level	Sugar concentration level	Impeller speed level	Air flow rate level
1	1	1	2	3
2	2	2	4	1
3	3	3	3	4
4	3	4	2	1

Since the cell was shown previously to be symmetrical about both the perpendicular bisector and the diagonal line (Sanwani,2006), 8 vertical axes were chosen to position the sensor. As depicted in Figure 6, axes 1 to 4 were positioned along the perpendicular bisector line, and axes 5 to 8 were distributed along the diagonal line.
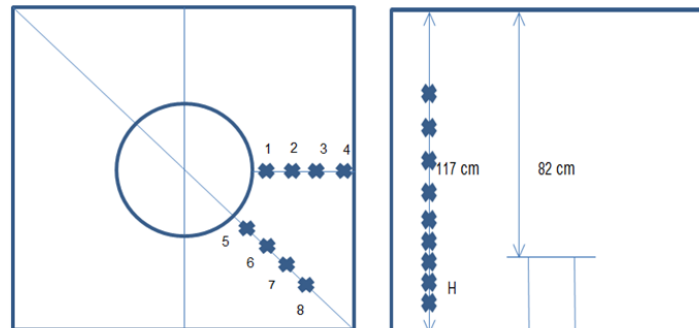
Figure 6. Top and side view of the measurement axes

Axes 1 and 5 were 40 cm from the centre of the cell ; axes 2 and 6, 51 cm;axes 3 and 7, 63 cm; and axes 4 and 8, 75 cm, respectively. These values were chosen for the convenience of fixing the metal tube on the cell while trying to keep the axes as evenly spaced as possible. On each axis, 15 locations were chosen as measurement points. With the stator plane as the reference position of 0 cm in the z (vertical) coordinate, the z coordinates (in

cm) of the 15 measurement positions on each axis were -29, -26, -23, -20, -17, -14, -11, -8, -5, -2, 1, 5, 10, 20, 30 cm, respectively. In order to capture the turbulence pattern, there were more measurement points under the stator plane than above, because the turbulence was greater under the stator plane.

Twenty experiments were carried out with the four hydrodynamic parameters set in accordance with Table 2 and Table 3. For each test, the kinetic energy fluctuation values at the measurement positions along the 8 axes were measured by the PVS and stored in the computer.

3.2 Experimental design for the Metso cell

Only three hydrodynamic parameters were selected for the Metso cell, namely, impeller speed, air flow rate and cell level. The L9 orthogonal array table(Keppel,1991) was chosen to design the orthogonal experiments such that 4 factors can be allowed to be varied across three levels, although only three factors were used. Table 4 lists the values at each level for each of the three parameters. Table 5 presents the 9 orthogonal experiments and Table 6 the 2 control group experiments.

Table 4. Levels for the three parameters in Metso cell

Level	Impeller speed as percentage of full speed (%)	Superficial gas flow rate J_g(cm/s)	Cell level as percentage of full height (%)
1	90	1.47	90
2	70	0.98	79
3	50	0.49	72

Table 5. Nine orthogonally designed experiments from L9

Experiment number	Impeller speed level	Gas flow rate level	Cell level
1	2	3	1
2	3	2	1
3	1	1	1
4	3	3	2
5	2	1	2
6	1	2	2
7	1	3	3
8	2	2	3
9	3	1	3

Table 6. Two control group tests

Experiment number	Impeller speed as percentage of full speed(%)	Superficial Gas flow rate J_g(cm/s)	Cell level as percentage if full height(%)
1	60	1.22	90
2	80	0.81	79

Despite the presence of feed and discharge points on opposite sides of the cell, the flow pattern inside the cell could still be assumed to be approximately symmetrical as the cell was operating in batch mode (no feed or discharge flow). Therefore, 4 vertical axes were chosen as the measurement axes, with 15 measurement positions at different heights on each axis. The distances of the axes from the center of the cell were 32, 44, 57 and 69 cm, respectively, and the height of the measurement points on each cell were 2, 5, 8, 11, 14, 17, 20, 23, 26, 29, 32, 42, 52, 72 and 102 cm above the bottom of the cell, respectively, as shown in Figure 7. For each test in Table 5 or Table 6, the kinetic energy fluctuation data were recorded at all the measurement points using the PVS sensor and stored in the computer for later analysis.
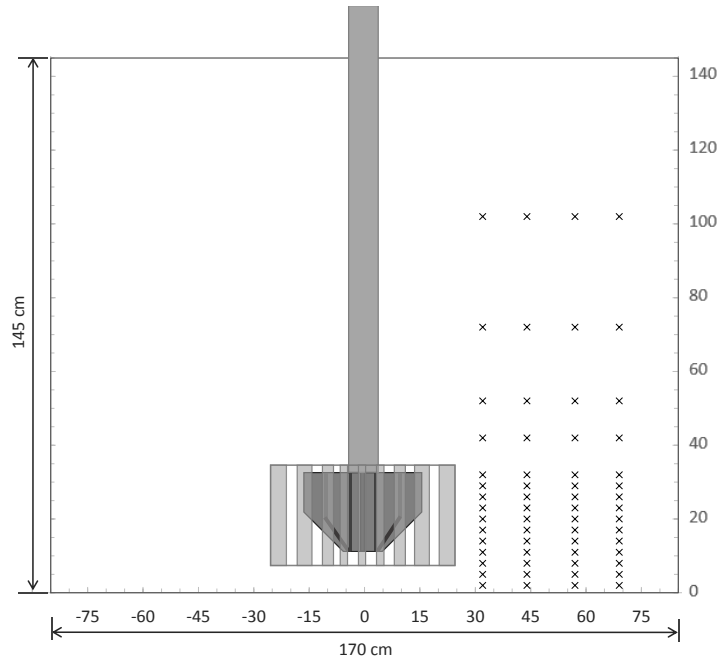
Figure 7 Measurement points in Metso cell

4. Data processing and modelling

4.1 JKMRC 3 m³ cell

4.1.1 Turbulence isosurface visualisation

The measured data were processed using MATLAB code. The kinetic energy fluctuation value at any position in the flotation cell was obtained by interpolating the measured data on the 8 axes and then mapping the measured region to unmeasured regions based on symmetrical mappings. A grid was meshed in the polar coordinate system in that $(r, \theta, z) \in \{[40,75], [0^o, 45^o], [-29,30]\}$. MATLAB function *interp3* was employed to perform the spline interpolation, the kinetic energy fluctuation value at any mesh point could then be obtained. Another grid was meshed in the Cartesian coordinate system in that $(x, y, z) \in \{\left[40cos\frac{\pi}{4}, 75\right], \left[0, 75sin\frac{\pi}{4}\right], [-29,30])\}$.

The kinetic energy fluctuation value at each grid point was obtained by interpolating the values of the 8 neighbouring grid points in the polar coordinate system using cubic splines. Then the MATLAB function *isosurface*, which was specifically designed for the Cartesian coordinate system, was used to draw the isosurface of a certain turbulence level.

Figure 8 depicts two turbulence isosurfaces for experiment 1, with the turbulence levels corresponding to 70% and 40% of the maximum turbulence level in this experiment. It can be seen that the isosurface of 40% peak turbulence value (in blue) stayed outside the isosurface of 70% peak turbulence value (in red), which reflects the natural structure of the turbulence distribution in the cell. The central part corresponds to the location of the stator where measurements are impossible.
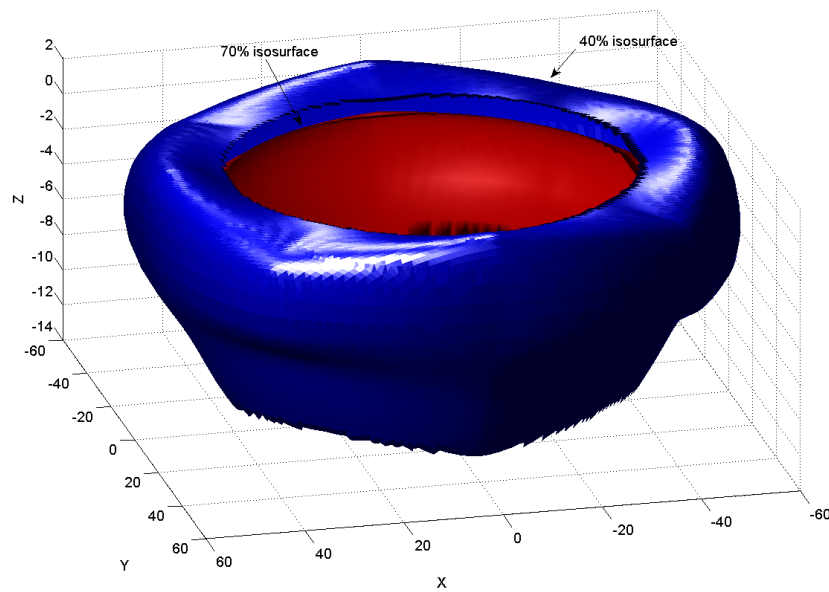
Figure 8. Two isosurfaces in experiment 1

4.1.2 Calculation of the turbulence zone volume

From Figure 8, it can be seen that the volume inside the 40% peak turbulence level isosurface is bigger than that inside the 70% peak turbulence level isosurface. The volume inside the isosurface of a certain turbulence level forms a turbulence zone. To calculate the volume of each turbulence zone, MATLAB code was developed. The idea was to vary θ from 0° to 45° in the polar coordinate system, and calculate the equipotential curve of the turbulence level on the plane defined by θ, as depicted in Figure 9. For small increments of θ, the volume between two equipotential curves could be calculated. By integral of all such volumes when θ increased from 0° to 45°, the turbulence zone volume V in the half quadrant could be obtained. Since the cell was geometrically symmetrical, the total volume was 8V.
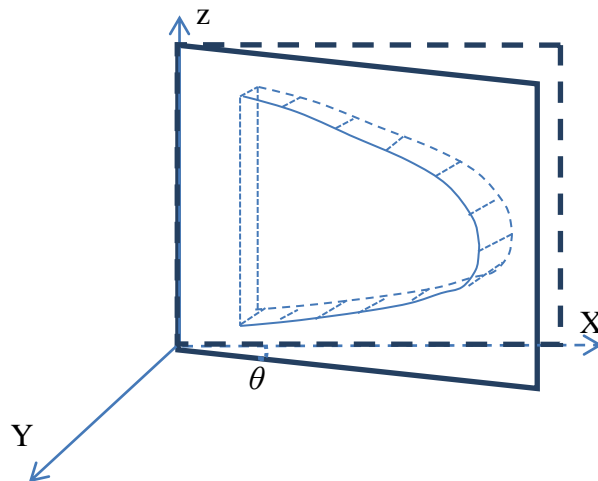

Figure 9. Calculation of volume between two equipotential curves

Figure 10 depicts a typical isosurface constructed by multiple equipotential curves when θ increased from 0° to 45°, drawn by MATLAB function *contourslice*. The dataset used was from experiment 1, and the turbulence level chosen was 70% of the peak turbulence level in experiment 1.
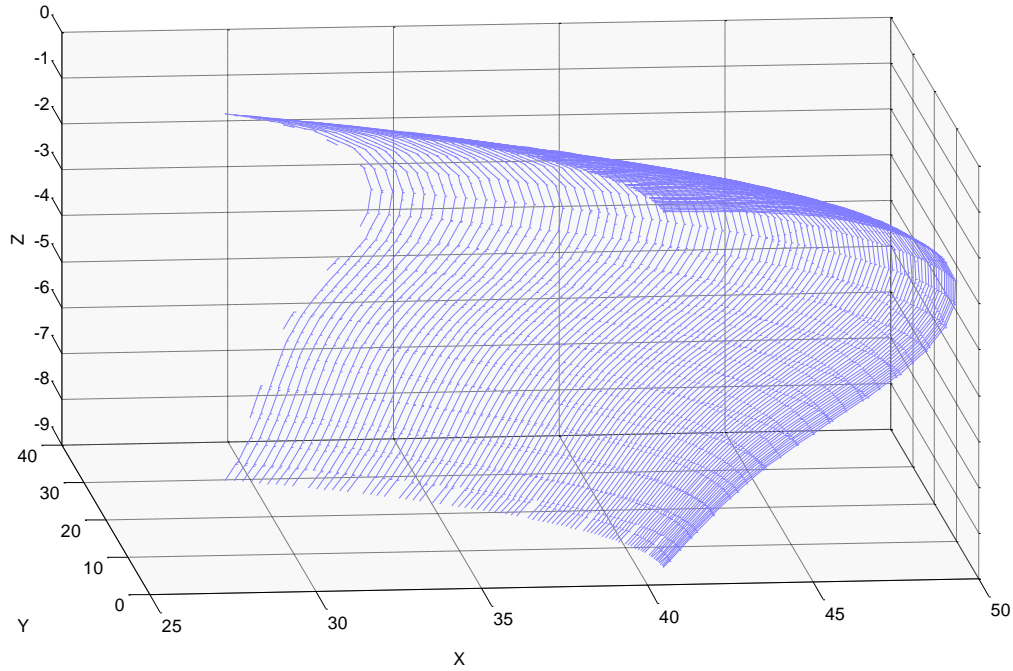
Figure 10. Typical isosurface constructed by equipotential curves

To establish a model for turbulence zone volume, volume values for all experiments had to be calculated first. As the peak turbulence value was different for each experiment, the maximum among the peak values was chosen as the benchmark maximum value T_{max}. For each experiment in the 16 orthogonal experiment group and the 4 control experiment group, the maximum achievable turbulence T_{local} was calculated and compared with T_{max}, and a percentage was calculated as $p=100\% \times (T_{local} / T_{max})$. Then for each experiment , turbulence zone volumes were calculated for all the multiples of 10% less than p. For example, if $p = 45\%$, then 40%, 30%, 20% and 10% turbulence zone volumes were calculated. The volumes were then divided by the total volume of the liquid inside the flotation cell to get a normalized volume V_p. Table 7 lists the calculation results for the normalized volumes.

Table 7. Normalized volumes calculated for all the experiments in JKMRC cell

Percentage(p)	90	80	70	60	50	40	30	20	10
Experiment number	Orthogonal experiments normalized volume (V_p) [10^{-2}]								
1						0.046	0.35	1.07	3.10
2		0.062	0.302	0.519	0.822	1.289	1.98	7.49	10.73
3	0.013	0.191	0.575	0.732	1.103	1.704	5.50	9.50	15.27
4			0.006	0.050	0.199	0.438	0.90	1.70	4.93
5	0.004	0.054	0.171	0.420	0.836	1.457	2.44	4.11	19.89
6				0.001	0.047	0.212	0.62	1.40	3.22
7			0.000	0.050	0.221	0.550	1.12	1.97	4.48
8	0.035	0.144	0.481	0.651	1.036	1.587	2.44	12.93	13.36
9	0.032	0.118	0.525	0.713	1.141	1.845	3.05	19.24	16.90
10			0.003	0.042	0.194	0.507	1.07	2.13	19.12
11					0.014	0.119	0.41	1.02	2.50
12		0.001	0.026	0.126	0.366	0.791	1.49	2.81	15.15
13			0.024	0.187	0.512	0.919	1.56	3.38	13.00
14		0.011	0.202	0.562	1.096	1.768	2.71	7.43	15.96
15			0.018	0.201	0.565	1.009	1.66	2.95	12.99
16					0.003	0.090	0.38	0.97	2.40
	Control group experiments normalized volume(V_p) [10^{-2}]								
1		0.0007	0.0326	0.1465	0.4077	0.8730	1.58	2.87	6.66
2	0.0395	0.1124	0.4018	0.6846	1.1690	1.9310	3.03	16.20	15.44
3	0.0005	0.0195	0.0804	0.2296	0.5124	0.9987	1.71	5.77	5.89
4				0.0558	0.1990	0.4590	0.88	1.59	15.21

4.1.3 Modelling of turbulence zone volume

For each experiment in Table 7, an exponential curve can be fitted to correlate the normalized volume and the percentage, i.e. $V_p = ae^{-bp}$. Figure 11 depicts exponential curves from several experiments of the orthogonal design.
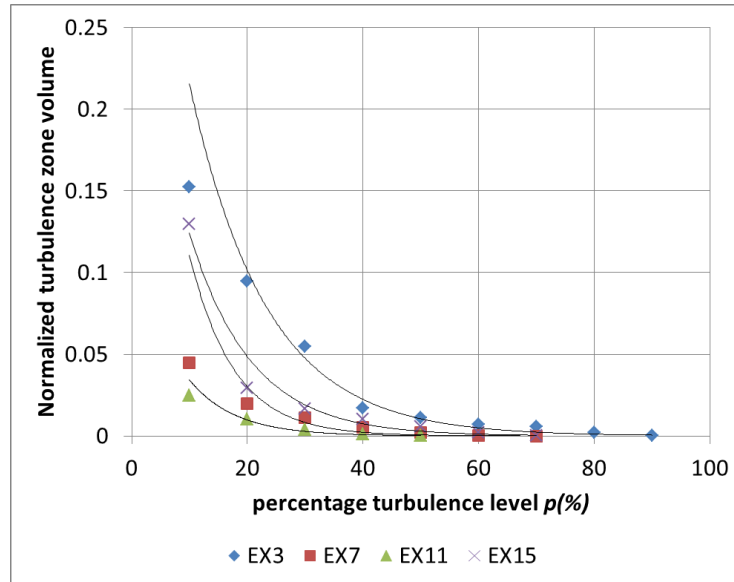

Figure 11. Exponential correlation between turbulence level and turbulence zone volume (JKMRC cell) for experiments 3, 7, 11 and 15

Table 8 lists the fitted parameters a, b as well as the goodness of fit, R^2.

Table 8. Fitted parameters a, b and R^2 for the JKMRC cell

Parameters	a	b	R²
Experiment number	Orthogonal experiments' parameters		
1	0.149	13.732	0.973
2	0.220	6.734	0.962
3	0.458	7.545	0.911
4	0.175	10.180	0.955
5	0.472	8.957	0.932
6	0.278	14.363	0.900
7	0.406	12.986	0.829
8	0.318	6.897	0.953
9	0.472	7.464	0.952
10	0.574	12.815	0.953
11	0.120	12.533	0.961
12	0.600	11.807	0.921
13	0.302	9.210	0.953
14	0.518	8.847	0.903
15	0.317	9.370	0.926
16	0.209	15.646	0.909
	Control group parameters		
1	0.431	11.193	0.874
2	0.420	7.311	0.970
3	0.459	10.347	0.890
4	0.227	9.978	0.949

Clearly in the model of $V_p = ae^{-bp}$, parameter a represents the normalized volume when p equals to zero, which is the proportion of the cell with turbulence essentially above zero (rather than laminar).   This does not preclude

the scenario where the zone falls outside the perimeter of the wall. Parameter *b* indicates how fast the turbulence zone volume expands as the minimum turbulence level within the zone decreases. To analyse how different hydrodynamic parameters affect *a* and *b*, a range analysis was applied to indicate the level of influence of each hydrodynamic parameter upon *a* and *b*. There were four hydrodynamic parameters, namely cell water level, viscosity, impeller speed and air flow rate. Of these, viscosity was varied by adding different amount of sugar to the water. However, as the temperature changed between different experiments, viscosity could not be controlled accurately. Therefore an average viscosity was used for each level of sugar concentration. Table 9 shows the average viscosity at each sugar level. In Table 9, the viscosity value for each sugar level was calculated by averaging the viscosity values of the sugary solution in the four experiments with this sugar level, also taking into consideration the recorded temperatures for these experiments.

Table 9. Viscosity and sugar level

Sugar level	1	2	3	4
Viscosity (mPa.s)	0.92	0.86	0.88	0.97

The range analysis results are displayed in Table 10. The K_i value indicates the average contribution of the factor at its ith level to the normalized volume, and range indicates the biggest difference between the four K_i values.

Table 10. Range analysis results for experiments in JKMRC cell

Factor	Cell water level	Viscosity	Impeller speed	Air flow rate
	Influence on parameter *a*			
K1	0.42	0.25	0.19	0.34
K2	0.40	0.37	0.44	0.41
K3	0.33	0.37	0.33	0.32
K4	0.25	0.41	0.44	0.33
Range	0.17	0.16	0.25	0.09
	Influence on parameter *b*			
K1	10.49	9.55	14.07	10.70
K2	10.69	10.80	11.95	10.73
K3	10.61	10.51	8.57	10.13
K4	10.48	11.42	7.69	10.71
Range	0.21	1.87	6.38	0.60

From the range values it can be seen that impeller speed had the biggest impact on both parameters *a* and *b;* therefore, it was the main factor determining the turbulence distribution. Cell water level and viscosity had similar impact on parameter *a* while air flow rate was the least influential. For parameter *b,* viscosity still was an important factor while the cell water level became the least influential after air flow rate.

To establish a mathematical model for the turbulence zone volume, the trend of K_i was analysed for each hydrodynamic factor to determine the possible functional form that could be used to approximate its influence on parameter *a* or *b*. A least square curve fitting was applied to determine the values of all parameters in the functions and finally a model was obtained as follows.

$$a = 5.105(IS - 0.108)(v^2 - 1.791v + 0.850)e^{\left(\frac{Jg-8.652}{5.236}\right)^2 - 1.717h} \tag{1}$$

$$b = -24.05(IS - 1.324)(v^2 - 1.708v + 1.160)e^{\left(\frac{Jg-0.931}{1.332}\right)^2 + \left(\frac{h+8.836}{14.384}\right)^2} \tag{2}$$

$$V_p = ae^{-bp} \tag{3}$$

In equations (1) and (2), *h* is the normalized cell water level against 110cm, and *IS* is the normalized impeller speed against 300 rpm. J_g is normalized superficial gas flow rate against 1cm/s and *v* is normalized viscosity against 1mPa.s. Parameter *p* is the percentage of the turbulence level. It should be noted that the model was built on the results from the 16 orthogonal experiments listed in Table 2. The accuracy of the model can be tested by predicting the turbulence zone volumes and compare the predictions to experimental results from the control group experiments in Table 3. To validate the model, V_p was calculated using the model for all the turbulence levels in each of the 20 experiments, with the 16 experiments in Table 2 as a reference. The model predicted results are plotted against the volumes calculated from the experimental data in Figure 12.
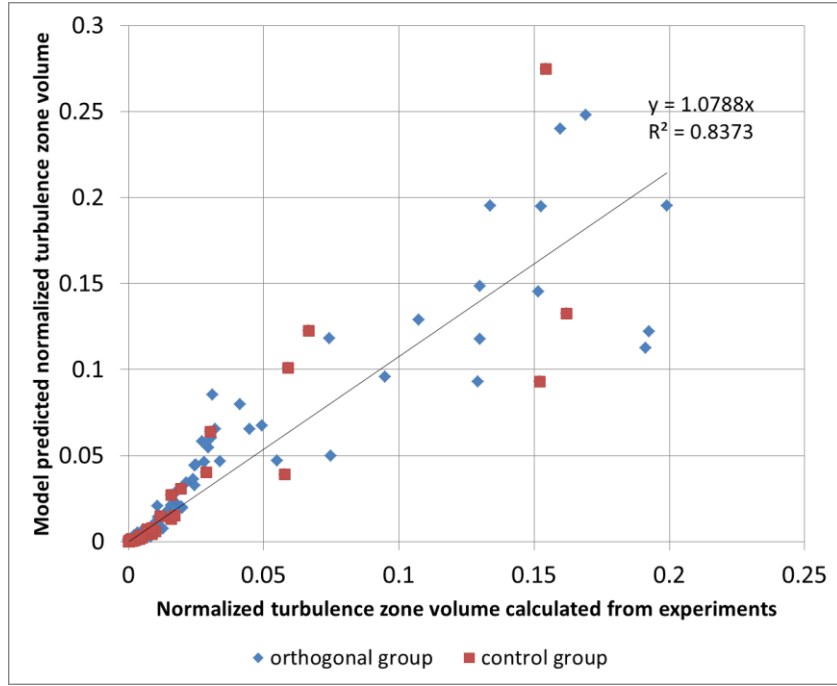
Figure 12. Model predicted volumes compared to experimental results (JKMRC cell)

In Figure 12 orthogonal experiments are represented by diamonds while control group experiments are represented by squares. A linear correlation was found between the model predictions and the calculated volumes from the experimental data. The overall goodness of fit was 0.8373, which is not very satisfactory. This may be caused by errors from the calculation of the turbulence zone volume when the turbulence level was very low and the turbulence zone reached far enough to be distorted by the walls. Another error causing factor was that the viscosity values in Table 9 were averaged values of four groups of tests, with each group having the same sugar concentration value. However, due to temperature changes, viscosity value was variable in each group. Therefore error was introduced into the viscosity data and propagated into the model.

4.2 Metso 3 m^3 RCS cell

4.2.1 Calculation of turbulence zone volume

In the cylindrical Metso cell, the turbulence zone volume could be calculated in a more straightforward way. Figure 13(a) depicts a colour map of turbulence intensity for orthogonal experiment 1. The turbulence intensity is displayed as the ratio of the maximum turbulence level. Figure 13(b) illustrates the algorithm used to calculate the turbulence zone volume defined by a typical contour line. The turbulence zone volume for this turbulence level would be equal to the volume of the revolved body when revolving the contour line around the z axis. It can be calculated by integrating the volume increment, which is the volume between the two cylinders in Figure 13(b), when r varies from the innermost to the outermost value.

$$V = \int_{r_{min}}^{r_{max}} 2\pi\, r h(r) dr \qquad (4)$$
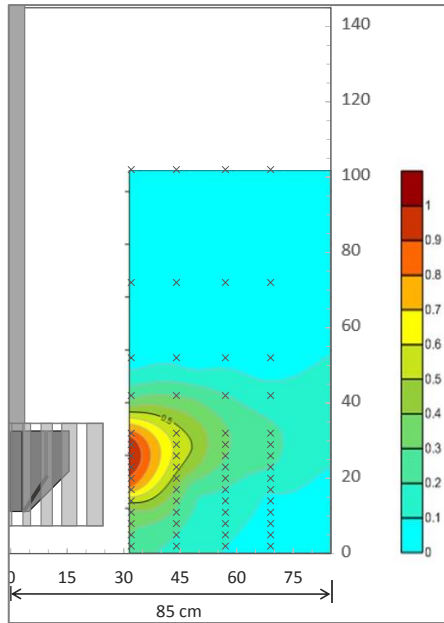
(a) Turbulence distribution
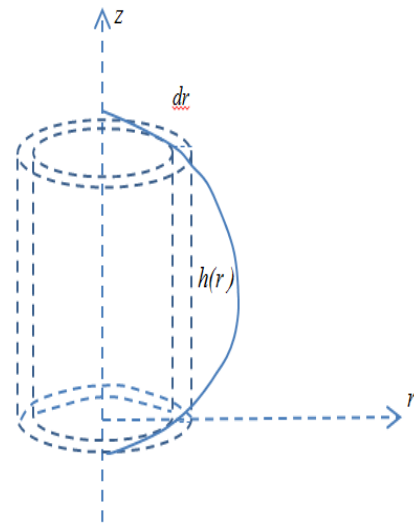
(b) How to calculate the volume increment

Figure 13. Contour lines and turbulence zone volume increment (Metso cell)

Similar to the calculations done for the JKMRC cell, turbulence zone volumes (normalized to total pulp volume) were calculated for turbulence levels at all multiples of 10% of the maximum measured turbulence level and for all the orthogonal and control group experiments. The results are listed in Table 11.

Table 11. Normalized volumes calculated for all the experiments in the Metso cell

Percentage (p)	90	80	70	60	50	40	30	20	10
Experiment number	Orthogonal experiments normalized volume (V_p) [10^{-2}]								
1					0.079	0.525	1.26	2.90	8.43
2						0.059	0.45	1.26	3.76
3			0.102	0.366	0.761	1.328	2.34	5.63	13.20
4					0.136	0.516	1.12	2.27	6.44
5			0.065	0.331	0.734	1.345	2.34	5.58	14.27
6	0.094	0.410	0.828	1.378	2.115	3.566	6.69	12.09	23.06
7	0.179	0.442	0.807	1.343	2.078	3.300	5.52	9.99	22.33
8				0.005	0.250	0.778	1.72	4.35	11.37
9					0.016	0.43	1.42	5.36	
	Control group experiments normalized volume （V_p） [10^{-2}]								
1					0.136	0.508	1.12	2.29	7.57
2	0.016	0.235	0.590	1.084	1.807	2.828	5.45	10.09	21.88

4.2.2 Modelling of turbulence zone volume

Similar to the modelling process done for the JKMRC cell, an exponential curve, $V_p = ae^{-bp}$, could be fitted for every experiment. Figure 14 depicts the exponential correlations for several orthogonal experiments.
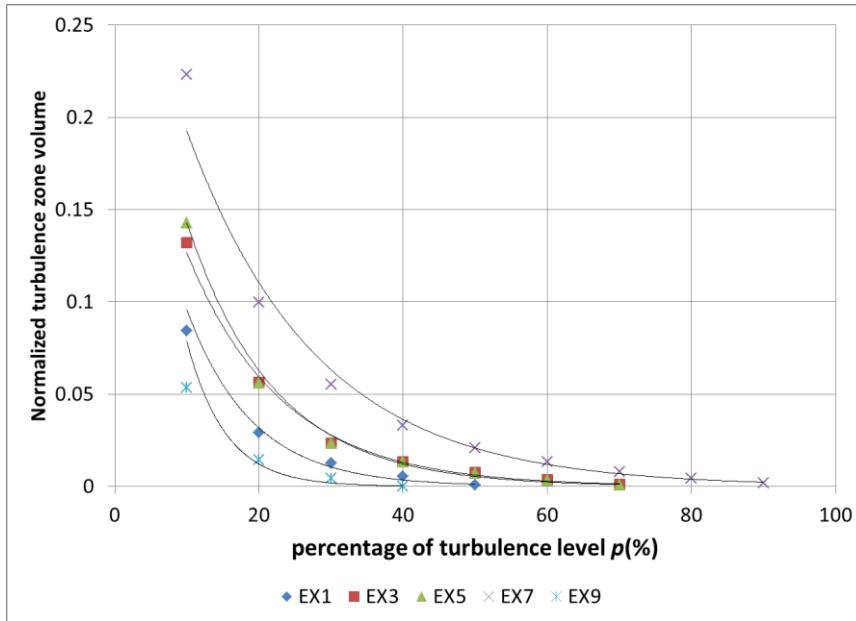
Figure 14. Exponential correlation between turbulence level and turbulence zone volume (Metso cell)

The fitted parameters *a* and *b* as well as goodness of fit, R^2, are listed in Table 12.

Table 12. Fitted parameters *a*, *b* and R^2 for Metso cell

Parameters	a	b	R^2
Experimental round	Orthogonal experiments parameters		
1	0.289	11.054	0.970
2	0.174	13.506	0.970
3	0.270	7.566	0.986
4	0.162	9.201	0.987
5	0.325	8.211	0.975
6	0.457	6.214	0.975
7	0.336	5.567	0.991
8	0.810	13.759	0.879
9	0.509	18.681	0.934
	Control group parameters		
1	0.186	9.542	0.988
2	0.603	7.600	0.914

Table 13 lists the range analysis results for the Metso cell experiments. It can be seen from the range analysis that the impeller speed again was the most important factor determining the turbulence distribution, followed by cell level and air flow rate.

Table 13. Range analysis results for experiments in Metso cell

Factor	Impeller speed	Air flow rate	Cell level
Influence on parameter *a*			
K1	0.387	0.282	0.215
K2	0.290	0.277	0.312
K3	0.160	0.278	0.310
Range	0.227	0.006	0.097
Influence on parameter *b*			
K1	7.11	10.13	9.80
K2	9.50	8.88	8.19
K3	11.25	8.85	9.86
Range	4.14	1.28	1.66

To establish a model for the turbulence zone volume, a trend analysis was applied to K_i values in Table 13 for each factor to determine the functional form that the model should adopt. Using least square minimisation curve fitting techniques, the model was determined as:

$$a = 0.0189(IS + 0.626)e^{(\frac{Jg+32.797}{12.617})^2 - 5.703h} \tag{5}$$

$$b = -0.212(IS - 1.269)e^{(\frac{Jg+41.491}{20.925})^2 + (\frac{h-0.819}{0.135})^2} \tag{6}$$

$$V_p = ae^{-bp} \tag{7}$$

In equations (5) and (6), *IS* is the normalized impeller speed against 420 rpm, J_g is the superficial gas flow rate normalized against 1cm/s and *h* is the normalized cell level against the full cell height of 145cm. To validate the model described in equations (5) to (7), V_p was calculated using the model for all the turbulence levels in all the 11 experiments. The model predicted results are plotted against the volumes calculated from the experimental data in Figure 15.
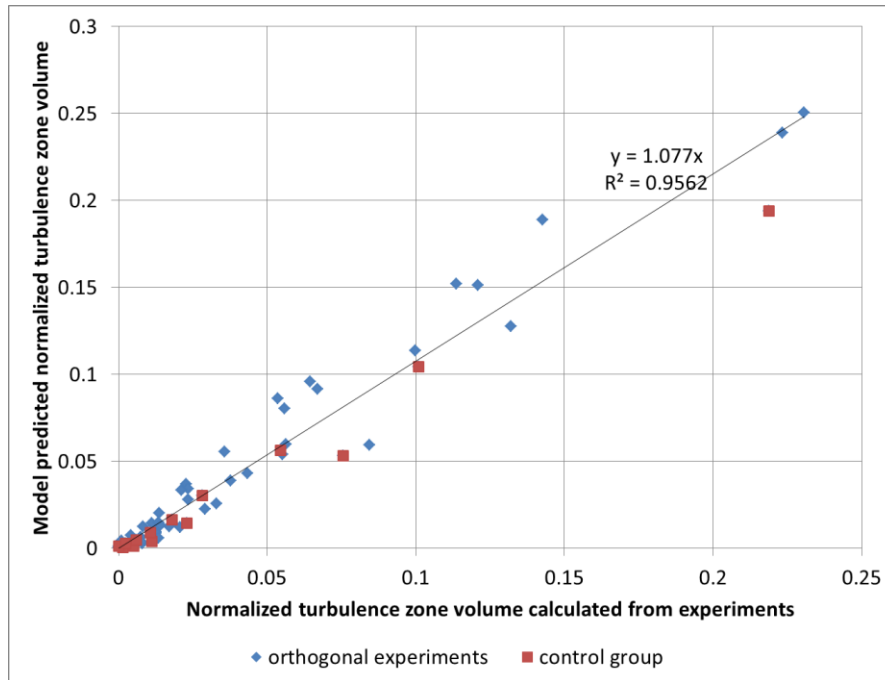

Figure 15. Model predicted volumes compared to experimental results (Metso cell)

In Figure 15 orthogonal experiments are represented by diamonds while control group experiments are represented by squares. A linear correlation was found between the model predictions and the calculated volumes from the experimental data. The overall goodness of fit was 0.9562, which is quite satisfactory.

5. Conclusions

The PVS has been proved to be an accurate and robust tool for turbulence measurement in flotation cells (Meng, Xie, *et al.*,2014; Meng, Tabosa, *et al.*,2014). The PVS in this study was firstly applied to a sugary water-air two phase mixture in a 3 m³ JKMRC pilot cell, using an orthogonal experimental design with 16 experiments, and then to a 3 m³ Metso RCS flotation test rig, using an orthogonal experimental design with 9 experiments.

The results from the experiments in these two cells have shown that turbulence zone volumes can be predicted through modelling. For each cell, an exponential model $V_p = ae^{-bp}$ was developed to predict the normalized turbulence zone volume V_p as a function of turbulence level, p. Parameter a in the model represents theg the proportion of the cell with turbulence essentially above zero (rather than laminar), while parameter b indicates how fast the turbulence zone volume expands as the turbulence level within the volume decreases. From range analysis impeller speed was seen to be the most important factor affecting a and b in both cells. For the Metso cell, the cell level had the second important influence on a and b; the air flow rate was the least influential factor. However, the JKMRC cell showed a more complicated influential pattern of the factors. For parameter a, the cell level was the second important factor which went before viscosity and air flow rate; but for parameter b, the viscosity became the second important which went before air flow rate, with cell level becoming the least important factor. The model established for the JKMRC cell can give predictions for the turbulence zone volume with moderate accuracy, while the model for the Metso cell can give fairly good predictions for both the orthogonal and the control group experimental conditions. The moderate accuracy of the JKMRC model may arise from the more complicated algorithm used for calculating the volumes because of the turbulence zone being distorted by the walls and viscosity not being constant due to observed temperature changes between the different experiments. Despite that, both of the models can provide important information about the turbulence distribution and how it changes as a function of flotation cell design and operation to enable the turbulence distribution to be incorporated into flotation rate models. This paper has also demonstrated techniques that can be used to transform localised turbulence measurements into global parameters to represent the overall turbulence distribution in a cell.

An understanding of the influences of all the hydrodynamic factors upon turbulence is crucial to enable optimisation of the flotation process. With this knowledge, the optimum combination of parameters for running flotation cells may be found to allow metallurgists to increase the recovery of minerals. Because turbulence has a significantly different effect on particles of different size, it is likely that the optimum set of conditions will vary with changes in the particle size of the feed. Further work is needed in this field.

References

Balaras, E.& Benocci, C. (1994) (Book)Applications of Direct and Large Eddy Simulation.Edited by Published by North Atlantic Treaty Organization. Advisory Group for Aerospace Research and Development. page

Brennan, M. S., Fry, M., Narasimha, M.& Holtham, P. N. (2007). *Water velocity measurements inside a hydrocyclone using an Aeroprobe & Comparison with CFD predictions,* Paper presented at the 16th Australasian Fluid Mechanics Conference (AFMC), Gold Coast, Queensland, Australia. 1131-1136

Fallenius, K. (1987) Turbulence in flotation cells. *International Journal of Mineral Processing, 21*(1–2), 1-23.

Grant, I.& Smith, G. H. (1988) Modern developments in particle image velocimetry. *Optics and Lasers in Engineering, 9*(3–4), 245-264.

Keppel, G. (1991) (Book)Design and analysis: A researcher's handbook (3rd ed.).Edited by Published by Prentice-Hall, Inc. page

Lu, H., Rutland, C. J.& Smith, L. M. (2007) A priori tests of one-equation LES modeling of rotating turbulence. *Journal of Turbulence, 8*(37), 1-27.

Meng, J., Tabosa, E., Xie, W., Runge, K.& Holtham, P. (2014) *Development and application of a piezoelectric sensor for turbulence measurement in industrial flotation cells*, Proc. 12th AusIMM Mill Operators' Conference 2014. Townsville Queensland, Australia. 457-469.

Meng, J., Xie, W., Brennan, M., Runge, K.& Bradshaw, D. (2014) Measuring turbulence in a flotation cell using the piezoelectric sensor. *Minerals Engineering, 66-68*, 84-93.

Menter, F. R. (1993). Improved two-equation k-w turbulence model for aerodynamic flows, *NASA Technical Memorandum 103975*.Ames Research Center.California.

Morris, R. M.& Matthesius, G. A. (1988) Froth flotation of coal fines: The influence of turbulence on cell performance. *Journal of the South African Institute of Mining and Metallurgy, 88*(12), 385-391.

Morud, K. E.& Hjertager, B. H. (1996) LDA measurements and CFD modelling of gas-liquid flow in a stirred vessel. *Chemical Engineering Science, 51*(2), 233-249.

Ngoepe, N. N., Mainza, A. N., Govender, I., Bradshaw, D. J., Morrison, A. J.& Parker, D. J. (2013). *Tracking the motion of particle-bubble aggregates in flotation using PEPT,* Paper presented at the XXVI International Mineral Processing Congress - IMPC 2012 (ERA 2010 Rank A), New Delhi, India. Technowrites

Sanwani, E. (2006). *Measurement and modelling of gas dispersion characteristics in a mechanical flotation cell.* (PhD. Thesis), University of Queensland, Brsiabane, Queensland.

Schubert, H. (1999) On the turbulence-controlled microprocesses in flotation machines. *International Journal of Mineral Processing, 56*(1–4), 257-276.

Sherif, S. A. (1998) Hot-wire/film anemometry measurements in flows with heat transfer and signal correction. *ISA Transactions, 37*(3), 141-146.

Tabosa, E., Runge, K.& Holtham, P. (2012, 24-28 September, 2012) *Development and application of a technique for evaluating turbulence in a flotation cell*, Proc. XXVI International Mineral Processing Congress （IMPC2012）. New Delhi, India. 5377-5390.

Tabosa, E., Runge, K.& Duffy, K.-A. (2013, November 18-21, 2013) *Strategies for increasing coarse particle flotation in conventional flotation cells*, Proc. The 6th International Flotation Conference Cape Town, South Africa.

Tabosa, E., Runge, K.& Holtham, P. (2014, 20-24 October 2014) *The effect of cell hydrodynamics on flotation kinetics*, Proc. XXVII International Mineral Processing Congress - IMPC 2014. Santiago, Chile. 18-27.

Xia, J., Rinne, A.& Grönstrand, S. (2009) Effect of turbulence models on prediction of fluid flow in an Outotec flotation cell. *Minerals Engineering, 22*(11), 880-885.